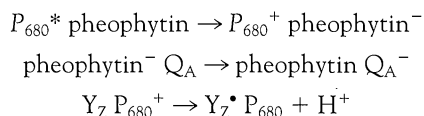# A Metalloradical Mechanism for the Generation of Oxygen from Water in Photosynthesis

Curtis W. Hoganson and Gerald T. Babcock*

In plants and algae, photosystem II uses light energy to oxidize water to oxygen at a metalloradical site that comprises a tetranuclear manganese cluster and a tyrosyl radical. A model is proposed whereby the tyrosyl radical functions by abstracting hydrogen atoms from substrate water bound as terminal ligands to two of the four manganese ions. Molecular oxygen is produced in the final step in which hydrogen atom transfer and oxygen-oxygen bond formation occur together in a concerted reaction. This mechanism establishes clear analogies between photosynthetic water oxidation and amino acid radical function in other enzymatic reactions.

Almost all of the molecular oxygen in the atmosphere has been released as a by-product of water oxidation during photosynthesis in plants and algae. In contrast with both chemical and electrochemical oxygen production, photosynthetic oxygen evolution proceeds with very little driving force and requires only moderate activation energies (1–3). Moreover, photosystem II turns over rapidly (up to 50 molecules of O_2 released per second) in spite of having to protect itself from photochemical oxidative damage. Although a number of models for the oxygen-evolving process have been proposed (2–4), no consensus has yet emerged.

Structural information about photosystem II is still limited by the lack of suitable crystals, but biochemical, spectroscopic, and kinetic studies have provided considerable insight into the catalytic center and its mechanism. The oxygen-evolving complex is made up of a redox-active tyrosine and a tetranuclear manganese cluster that binds substrate water and accumulates oxidizing equivalents. The S-state notation (5) identifies the number of oxidizing equivalents stored; O_2 is released on the transition from S_3 to S_4 to S_0. These oxidizing equivalents are generated when photon energy is absorbed and transferred to a primary electron donor, P_{680} (1). Upon photoexcitation of P_{680}, a series of electron transfer reactions between cofactors within the protein takes place:

$$P_{680}^* \text{ pheophytin} \rightarrow P_{680}^+ \text{ pheophytin}^-$$

$$\text{pheophytin}^- Q_A \rightarrow \text{pheophytin } Q_A^-$$

$$Y_Z P_{680}^+ \rightarrow Y_Z^\bullet P_{680} + H^+$$

The products are a plastosemiquinone anion radical, Q_A^-, and a neutral tyrosyl radical, $Y_Z^\bullet$, residing on Tyr^{161} of the D1

The authors are in the Department of Chemistry, Michigan State University, East Lansing, MI 48824–1322, USA.

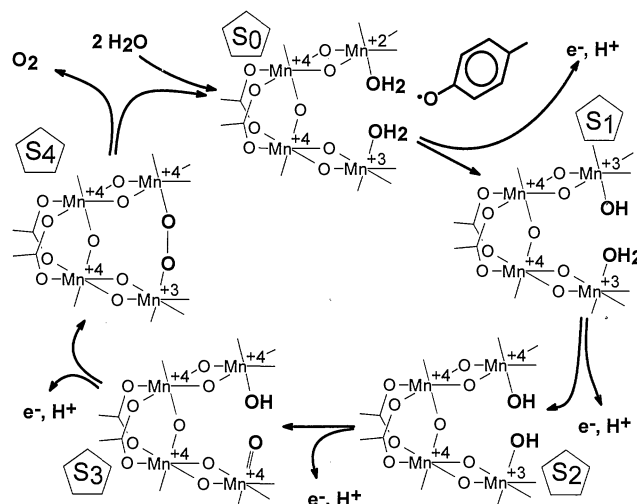*To whom correspondence should be addressed. E-mail: babcock@cemvax.cem.msu.edu

polypeptide (6). Reduction of $Y_Z^\bullet$ by the manganese cluster occurs in 50 to 1300 µs, depending on the S state.

Recent data give additional insight into the structure and function of the active site. Y_Z, in its reduced state, is probably hydrogen bonded to His^{190} (7). $Y_Z^\bullet$ has physical properties that are dependent on the integrity of the manganese cluster (8), consistent with its proximity (≤5 Å) to the metal center (9). A proposal for the structure of the manganese cluster shows the two di-µ-oxo manganese dimers connected at one end by one bridging oxo and two bridging carboxylato ligands (10, 11). Proton release to the surface of the protein is detectable in as little as 12 µs (12, 13), which is faster than the reduction time of $Y_Z^\bullet$. On the basis of these recent data and on parallels between photosystem II and the class of radical-containing metalloenzymes that metabolize oxygen or peroxide, we have proposed a metalloradical mechanism for oxygen evolution (8, 14, 15) (Fig. 1).

This model differs from previous proposals concerning the mechanism of water oxidation in two ways. First, the tyrosyl radical acts as a hydrogen atom abstractor (8, 9) rather than as a simple electron transfer cofactor (16). This enables the manganese cluster to remain electrically neutral, or nearly so, in all of its S states, rather than to accumulate positive charges as it becomes more oxidized (5). Upon its oxidation, Y_Z releases a proton to His^{190}, and this proton is ultimately delivered to the bulk aqueous phase. The reactions of protons and electrons are coupled on each S-state advancement, resulting in a requirement for only one set of bases for proton extraction and delivery to the aqueous phase, obviating the need for additional bases to bind several protons at once (13).

Second, dioxygen is postulated to form from water bound as terminal ligands to the manganese, not from bridging oxo ligands as in many earlier proposals (4, 17). The two manganese ions at the open end of the C-shaped cluster, 5.5 Å apart in the structure of Dau et al. (11), are rigidly held in a superstructure that is ideally suited to promote the formation of the O–O bond between terminal ligands. This has the advantage of minimizing nuclear motion within the manganese cluster and should enable a high catalytic rate. Precedence for terminal oxo collapse to dioxygen has come from study of model compounds (18). Recent data show that ^{18}O-labeled water exchanges into the binding sites in S_3 in less than one second (19). This rapid exchange is inconsistent with a bridging oxo origin for product O_2 (20).

Fig. 1. A model for the S-state cycle of the manganese cluster of photosystem II. For clarity, Y_Z is shown only in the S_0 state. Calcium and chloride ions are required for oxygen evolution activity (2, 57), particularly for the formation of the S_2 state, and their specific functions within the context of the metalloradical mechanism are considered in detail elsewhere (31).

We now consider the details of the hydrogen atom transfer reactions. We develop the model by considering the oxidation states of the manganese atoms explicitly and by proposing a mechanism for oxygen-oxygen bond formation that requires direct participation of the tyrosyl radical. This process has analogies to several enzymatic and nonenzymatic reactions.

Hydrogen Atom Abstractions

The overall reaction of four tyrosyl radicals and two water molecules to produce dioxygen is favorable by about 23 kcal per mole of O_2, as shown by the bond dissociation energies (21) (Scheme 1). Although the net reaction is exothermic, this scheme

$2 \times \{$	$H_2O \rightarrow$	$OH^{\bullet} + H^{\bullet}$	+119 kcal/mol $\}$	+238 kcal/mol
$2 \times \{$	$OH^{\bullet} \rightarrow$	$^{\bullet}O^{\bullet} + H^{\bullet}$	+102 kcal/mol $\}$	+204 kcal/mol
	$2\,^{\bullet}O^{\bullet} \rightarrow$	O_2	−119 kcal/ mol	−119 kcal/mol
$4 \times \{$	$H^{\bullet} + TyrO^{\bullet} \rightarrow$	$TyrOH$	−86.5 kcal/mol $\}$	−346 kcal/mol
$2 H_2O + 4\ TyrO^{\bullet}$	$\rightarrow$	$O_2 + 4\ TyrOH$		−23 kcal/mol

shows that hydrogen atom transfer to tyrosyl from free H_2O or $OH^{\bullet}$ is endothermic. In studies of model manganese compounds, however, the O-H bond dissociation energies of aquo and hydroxo ligands decrease considerably and are comparable to that of tyrosine (22–25) (Table 1). These results support the thermodynamic feasibility of hydrogen atom transfers within photosystem II as the mechanistic basis for water oxidation and O_2 evolution. They also identify essential functions of the manganese cluster in PSII in positioning water or hydroxide for effective hydrogen atom abstraction and in delocalizing oxidizing equivalents during the S-state progression.

We expect that the transfers of the oppositely charged electron and proton occur in a coupled process rather than sequentially. Electrostatic solvation affects reaction rates by contributing to the activation energies in ways that depend predictably on whether charges are separated, neutralized, or dispersed in the transition state (26). The transfer of a neutral particle between neutral species, as in a free-radical atom

transfer reaction, induces small changes in the solvation of the reacting molecules. Thus, the solvation energy remains more nearly constant across the reaction coordinate and contributes little to the activation energy. The activation energy for $Y_Z^{\bullet}$ reduction on the S_1 to S_2 transition is only 2.3 kcal/mol (27), which implies a low reorganization energy. This reaction also shows a substantial deuterium kinetic isotope effect [(28); but see (29)], which indicates that there is significant coupling of proton motion into the electron transfer coordinate associated with S-state advance, consistent with either a hydrogen atom transfer reaction or a proton-coupled electron transfer. The other S-state transitions show somewhat higher activation energies (27) and lower kinetic isotope effects (28–30), suggesting that additional nuclear motions occur simultaneously with the H atom transfer during these transitions. The kinetic competence of the proposed atom transfers in PSII has been established (31).

The S-State Cycle: The Stable S States

The metalloradical mechanism for the S-state cycle is shown in Fig. 1. Consensus is emerging on the Mn valences in most of the S states with data available from ultraviolet (UV) absorption (32), electron paramagnetic resonance (EPR) (33), and x-ray absorption near edge spectroscopy (XANES) (34–36) and provides the basis for the valence assignments. Data obtained by EPR shows that S_2 has an odd number of unpaired electrons. The S_1 and S_2 states have been the best characterized by XANES, and the most likely sets of manganese oxidation states are for S_1, $\{+3,+3,+4,+4\}$, and for S_2, $\{+3,+4,+4,+4\}$. The UV absorption changes on $S_1 \rightarrow S_2$ and $S_2 \rightarrow S_3$ are similar

(32) and, together with the XANES data of Ono et al. (34) and the lack of oxidizable amino acid side chains in the vicinity of the Mn cluster other than Y_Z (see below), justify the $\{+4,+4,+4,+4\}$ S_3 valence assignment (37). Data from XANES indicate oxidation of manganese on the $S_0 \rightarrow S_1$ transition (35), implying that the S_0 state is either $\{+3,+3,+3,+4\}$ or $\{+2,+3,+4,+4\}$. Although we favor the latter assignment in Fig. 1, experimentally these two S_0 valence sets appear to be close in energy (38). This near degeneracy most likely reflects the opposing effects of the arrangement of charged ligands to the cluster (see below), and the tendency of a $+2/+4$ dimer to convert to the $+3/+3$ state.

The two carboxylato-bridged manganese ions of the Dau et al. (11) model have anionic ligands that sum to a negative charge of eight [two carboxylates (−2) one oxo (−2) and four bridging oxos (−4)]. This environment should stabilize the +4 oxidation state, making these centers less strongly oxidizing (39), and we indicate that they remain in the +4 state throughout the S state cycle. In our view, these two atoms act to anchor the two catalytic manganese atoms at the open end of the cluster. The catalytic ions have fewer anionic ligands, although still enough to render the overall site neutral (15), and therefore the +4 oxidation states of these atoms are more strongly oxidizing. These two ions are oxidized from +3 to +4 on the transitions from S_1 to S_3. The oxidant created in the S_0 to S_1 transition is weaker than those created in the other S-state transitions (40), leading to our assignment of this transition as oxidation from +2 to +3 at a catalytic ion in Fig. 1.

Water binds at two sites that differ in their rates of $H_2^{16}O/H_2^{18}O$ exchange. Results by mass spectrometry show that one oxygen atom exchanges in less than 25 ms and the other in 500 ms in both the S_2 and S_3 states (19). This asymmetry in the water binding sites may be due to differences in ligation of the catalytic manganese ions— only one histidine (41) and only one chloride ion (42) are believed to be part of the manganese cluster—or to differences in protonation. Protonation is expected to enhance the rate of exchange (43).

The Oxygen-Forming Reaction

On the S_3 to S_4 to S_0 transition, an oxygen-oxygen bond is formed, dioxygen is released, and water rebinds to the manganese complex. The overall process occurs in 1 ms with an activation energy of only 9.6 kcal/mol. The S_4 state has not been observed. We now consider three mechanistic possibilities for the chemistry that occurs during this process.

Table 1. O-H Bond dissociation energies (BDE, kcal/mol) of model manganese compounds. Abbreviations: bpy is 2,2'-bipyridyl; L is 1,3-bis(3,5-di-X-salicylamino)propane; L′ is 2-hydroxy-1,3-bis(3,5-di-X-salicylamino)propane; X is H, Cl, or t-butyl.

Compound	Position	BDE	Ref.
$HMnO_4^-$	Terminal	83	(22)
$Mn_2(III,III)(\mu\text{-}O, \mu\text{-}OH)bpy_4{}^{+3}$	Bridging	84	(23)
$Mn_2(III,IV)(\mu\text{-}O, \mu\text{-}OH)L_2$	Bridging	76–79	(23)
$Mn_2(III,III)\ L'_2OH_2$	Terminal	82–89	(24)

1) The S_3 to S_4 transition has often been considered to be a manganese-centered oxidation. This would advance one manganese atom to the $+5$ oxidation state. In six-coordinate manganese, which is the likely ligand environment in PSII (44, 45), studies of model compounds indicate that the $+5$ state is rare (46) and highly oxidizing (47). Accordingly, we conclude that the $+5$ oxidation state of manganese is unlikely to be formed in PSII in a reaction with $Y_Z^\bullet$.

2) Other models have assigned the transition of S_3 to S_4 as a one-electron oxidation of a manganese ligand. Oxidation of a water or hydroxo ligand to produce an oxygen-centered radical without delocalization of the oxidizing equivalent into the manganese cluster can be ruled out by comparing the bond dissociation energy of tyrosine with those of water (Scheme 1) and hydroxide ion (109 kcal/mol) (48). In principle, tyrosine or tryptophan could be oxidized, but there are no indications that either are ligands to manganese (7, 49). One-electron oxidation of a histidine side chain is unlikely (50), and models that invoke histidine oxidation in PSII have not been substantiated (9). Thus, one-electron oxidation of a ligand is improbable on $S_3 \to S_4 \to S_0$ or, for that matter, on any of the S state transitions.

3) An alternate description of the S_3 to S_4 transition is as a two-electron oxidation of substrate ligands derived from water to produce a peroxide species bound to manganese (Fig. 1). As on the other S-state transitions, $Y_Z^\bullet$ abstracts a hydrogen atom, but now this reaction occurs in concert with the formation of an oxygen-oxygen bond and the reduction by one electron of one of the manganese ions. To complete the S-state cycle, the manganese-peroxo bonds cleave, releasing the dioxygen product and allowing water to bind to the newly vacated coordination sites. Although the S_4 state is indicated as a discrete intermediate, we expect that its lifetime will be so short as to preclude its detection.

The reaction that produces S_4 can be thought of as two reactions occurring simultaneously. The first is a hydrogen atom transfer that produces a manganese-bound oxyl radical and the second is the addition of the oxyl radical to the terminal oxo ligand of a second manganese ion. Because the manganese oxo bond has multiple bond character, the second step is analogous to the addition of a free radical to a double bond, familiar in organic and polymer chemistry. The overall reaction can be close to isoenergetic because two covalent bonds are formed and two are broken.

The structure of the manganese cluster and its proximity to Y_Z allow five atomic orbitals on the reactant atoms that partici-

pate in the reaction to overlap in the postulated transition state (Fig. 2). In the reactant and product conformations, these orbitals make two covalent bonds, and one unpaired electron occupies a nonbonding orbital. In the transition state, the electrons occupy delocalized molecular orbitals, giving partial bonds between adjacent atoms. The five orbitals constitute an odd-alternant structure in which resonance significantly lowers the energy of the transition state. The unpaired electron is then found mainly on the phenoxyl radical, the oxygen from which the hydrogen atom is abstracted, and the manganese atom. Thus, although there is no oxyl radical intermediate, the transition state does have some oxyl radical character. A similar system of five orbitals occurs in many base-promoted elimination reactions, such as the dehydrohalogenation of 2-phenylethyl-halides, which also occur concertedly rather than through a carbanion intermediate (51).

In this mechanism, O–O bond formation is fully allowed with respect both to conservation of spin angular momentum and to conservation of orbital symmetry. The model specifies that reduction of $Y_Z^\bullet$ occurs simultaneously with formation of the O–O bond. This prediction neatly accounts for the observation that $Y_Z^\bullet$ reduction and O_2 release occur with the same rates (52). Moreover, the geometric constraints implied by the concerted atom transfers that occur during the $S_3 \to S_4 \to S_0$ transition suggest that the kinetics of $Y_Z^\bullet$ reduction and O_2 release should be quite sensitive to minor structural perturbations, which rationalizes the substantial decrease in $Y_Z^\bullet$ reduction rate on the O_2-forming step when polypeptides peripheral to PSII are depleted
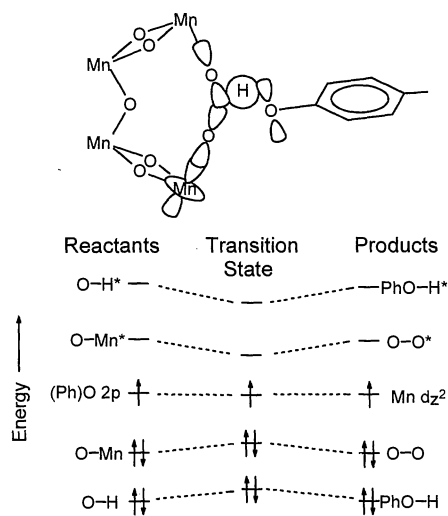
or when calcium is replaced by strontium (53).

A theoretical analysis of activation energies related to oxygen evolution (54) shows that peroxide can be formed most readily when the solvent reorganization energy is minimized using two one-electron oxidants, one of which accepts a proton in addition to an electron, as does the tyrosyl radical in our model. Similar energetic considerations govern the kinetics of bond formation and cleavage in other enzymatic redox reactions. Mechanisms similar to the one we propose here for PSII that use two redox cofactors, one copper atom and one hydrogen-abstracting tyrosyl or modified tyrosyl radical, have recently been proposed for dopamine-β-monooxygenase (55) and galactose oxidase (56).

Models for photosynthetic oxygen evolution must take into account several facts. The process operates in a low dielectric medium and with a low driving force. The former condition requires the cluster to be electrically neutral, or nearly so, while the latter, together with the low activation energies measured for $Y_Z^\bullet$ reduction, require that these reactions occur as electrically neutral reactions. Hydrogen atom transfers to $Y_Z^\bullet$ satisfy these requirements. The concerted radical mechanism proposed for the O-O bond forming step also enables a low activation energy and it avoids the intermediacy of a high-energy, uncontrollably reactive substrate free radical.

Fig. 2. Atomic orbitals (above) and molecular orbital diagram (below) showing the oxygen bond formation reaction. Only the orbitals undergoing the greatest changes during the reaction are shown.

REFERENCES AND NOTES

1. B. A. Diner and G. T. Babcock, in *Oxygenic Photosynthesis: The Light Reactions*, D. R. Ort and C. F. Yocum, Eds. (Kluwer, Dordrecht, Netherlands, 1996), pp. 213–247.
2. R. J. Debus, *Biochim. Biophys. Acta* **1102**, 269 (1992); H. T. Witt, *Ber. Bunsenges. Phys. Chem.* **100**, 1923 (1996).
3. R. D. Britt, in *Oxygenic Photosynthesis: The Light Reactions*, D. R. Ort and C. F. Yocum, Eds. (Kluwer, Dordrecht, Netherlands, 1996), pp. 137–164.
4. V. K. Yachandra, K. Sauer, M. P. Klein, *Chem. Rev.* **96**, 2927 (1996).
5. B. Kok, B. Forbush, M. McGloin, *Photochem. Photobiol.* **11**, 457 (1970).
6. B. A. Barry and G. T. Babcock, *Proc. Natl. Acad. Sci. U.S.A.* **84**, 7099 (1987); R. J. Debus, B. A. Barry, I. Sithole, G. T. Babcock, L. McIntosh, *Biochemistry* **27**, 9071 (1988).
7. A. Chu, A. P. Nguyen, R. J. Debus, *Biochemistry* **34**, 5839 (1995).
8. C. Tommos et al., *J. Am. Chem. Soc.* **117**, 10325 (1995); G. T. Babcock et al., *Acta Chem. Scand.* **51**, 533 (1997).
9. M. L. Gilchrist Jr., J. A. Ball, D. W. Randall, R. D. Britt, *Proc. Natl. Acad. Sci. U.S.A.* **92**, 9545 (1995); X.-S. Tang, D. W. Randall, D. A. Force, B. A. Diner, R. D. Britt, *J. Am. Chem. Soc.* **118**, 7638 (1996).
10. V. K. Yachandra, et al., *Science* **260**, 675 (1993).
11. H. Dau et al., *Biochemistry* **34**, 5274 (1995).
12. M. Haumann and W. Junge, *Biochemistry* **33**, 864 (1994).
13. _____, in *Oxygenic Photosynthesis: The Light Reactions*, D. R. Ort and C. F. Yocum, Eds. (Kluwer, Dordrecht, Netherlands, 1996), pp. 165–192.

14. C. W. Hoganson et al., Photosyn. Res. 46, 177 (1995).
15. G. T. Babcock, in Photosynthesis: From Light to Biosphere, P. Mathis, Ed. (Kluwer, Dordrecht, Netherlands, 1995), vol. 2, pp. 209–215.
16. ———, et al., Biochemistry 28, 9557 (1989).
17. G. W. Brudvig and R. H. Crabtree, Proc. Natl. Acad. Sci. U.S.A. 83, 4586 (1986); J. B. Vincent and G. Christou, Inorg. Chim. Acta 136, L41 (1987); V. L. Pecoraro, in Manganese Redox Enzymes, V. L. Pecoraro, Ed. (VCH, New York, 1992), pp. 197–231.
18. J. A. Gilbert et al., J. Am. Chem. Soc. 107, 3855 (1985); F. P. Rotzinger et al., ibid. 109, 6619 (1987); Y. Naruta, M. Sasayama, T. Sasaki, Angew. Chem. Int. Ed. 33, 1839 (1994).
19. J. Messinger, M. Badger, T. Wydrzynski, Proc. Natl. Acad. Sci. U.S.A. 92, 3209 (1995); J. Messinger, M. Badger, T. Wydrzynski, in Photosynthesis: From Light to Biosphere, P. Mathis, Ed. (Kluwer, Dordrecht, Netherlands, 1995), vol. 2, pp. 283–286.
20. Kinetic inertness to substitution of the bridging oxo atoms in $Mn_2(III,IV)(\mu-O)_2$ in superoxidized manganese catalase has been suggested as the basis for inactivity of this oxidation state; G. S. Waldo, S. Yu, J. E. Penner-Hahn, J. Am. Chem. Soc. 114, 5869 (1992); S. Khangulov, M. Sivaraja, V. V. Barynin, G. C. Dismukes, Biochemistry 32, 4912 (1993); M. Shank, V. Barynin, G. C. Dismukes, ibid. 33, 15433 (1994).
21. J. Lind, X. Shen, T. E. Eriksen, G. Merenyi, J. Am. Chem. Soc. 112, 479 (1990); J. A. Kerr, in Handbook of Chemistry and Physics (Chemical Rubber, Cleveland, OH, ed. 77, 1996), pp. 9–51.
22. K. A. Gardner and J. M. Mayer, Science 269, 1849 (1995).
23. M. Baldwin and V. L. Pecoraro, J. Am. Chem. Soc. 118, 11325 (1996).
24. M. T. Caudle and V. L. Pecoraro, ibid. 119, 3415 (1997).
25. M. R. A. Blomberg et al., ibid., in press.
26. C. K. Ingold, Structure and Mechanism in Organic Chemistry (Cornell Univ. Press, Ithaca, NY, ed. 2, 1969), pp. 457–463 and 681–686; A. Pross, Theoretical and Physical Principles of Organic Reactivity (Wiley, New York, 1995).
27. H. Koike, B. Hanssum, Y. Inoue, G. Renger, Biochim. Biophys. Acta 893, 524 (1987); G. Renger and B. Hanssum, FEBS Lett. 299, 28 (1992).
28. N. Lydakis-Simantiris, C. W. Hoganson, D. F. Ghanotakis, G. T. Babcock, in Photosynthesis: From Light to Biosphere, P. Mathis, Ed. (Kluwer, Dordrecht, Netherlands, 1995), vol. 2, pp. 279–282; N. Lydakis-Simantiris, D. F. Ghanotakis, G. T. Babcock, Biochim. Biophys. Acta, in press.
29. O. Bögershausen, M. Haumann, W. Junge, Ber. Bunsenges. Phys. Chem. 100, 1987 (1996); M. Karge, K.-D. Irrgang, G. Renger, Biochemistry 36, 8904 (1997).
30. M. Karge et al., FEBS Lett. 378, 140 (1996).
31. C. Tommos and G. T. Babcock, Acct. Chem. Res., in press.
32. J. P. Dekker, H. J. Van Gorkom, J. Wensink, L. Ouwehand, Biochim. Biophys. Acta 767, 1 (1984); J. Lavergne, ibid. 1060, 175 (1991); M. Haumann, W. Drevenstedt, M. Hundelt, W. Junge, ibid. 1273, 237 (1996); H. Kretschmann, E. Schlodder, H. T. Witt, ibid. 1274, 1 (1996).
33. G. C. Dismukes and Y. Siderer, Proc. Natl. Acad. Sci. U.S.A. 78, 274 (1981); A. Haddy, W. R. Dunham, R. H. Sands, R. Aasa, Biochim. Biophys. Acta 1099, 25 (1992).
34. T. Ono et al., Science 258, 1335 (1992).
35. P. J. Riggs, C. F. Yocum, J. E. Penner-Hahn, R. Mei, J. Am. Chem. Soc. 114, 10650 (1992).
36. T. A. Roelofs et al., Proc. Natl. Acad. Sci. U.S.A. 93, 3335 (1996).
37. Roeloffs et al. (36) argued against a Mn valence change on $S_2 \to S_3$, and Yachandra et al. (4) have proposed that one-electron oxidation of the bridging oxo group (or groups) occurs. However, a similar bridging oxyl ligand formulation for intermediate X in ribonucleotide reductase has been discarded recently in favor of iron-centered oxidation in the binuclear cluster in that enzyme (58) and the free energy

38. necessary to generate an oxyl may be prohibitively high (48). Accordingly, we disfavor an oxyl formulation for S_3.
38. P. J. Riggs-Gelasco, R. Mei, C. F. Yocum, J. E. Penner-Hahn, J. Am. Chem. Soc. 118, 2387 (1996); see also, J. Messinger, J. H. A. Nugent, M. C. W. Evans, Biochemistry, in press.
39. J.-J. Girerd, in Photosynthesis: From Light to Biosphere, P. Mathis, Ed. (Kluwer, Dordrecht, Netherlands, 1995), vol. 2, pp. 217–222.
40. I. Vass and S. Styring, Biochemistry 30, 830 (1991).
41. X.-S. Tang et al., Proc. Natl. Acad. Sci. U.S.A. 91, 704 (1994).
42. K. Lindberg, T. Vänngård, L.-E. Andréasson, Photosyn. Res. 38, 401 (1993).
43. K. W. Kramarz and J. R. Norton, Prog. Inorg. Chem. 42, 1 (1994).
44. V. L. Pecoraro, Photochem. Photobiol. 48, 249 (1988).
45. D. W. Randall et al., J. Am. Chem. Soc. 117, 11780 (1995).
46. F. A. Cotton and G. Wilkinson, Advanced Inorganic Chemistry (Wiley, New York, ed. 5, 1988), p. 707; N. N. Greenwood and A. Earnshaw, Chemistry of the Elements (Pergamon, Oxford, 1984), p. 1228; R. Manchandra, G. W. Brudvig, R. H. Crabtree, Coord. Chem. Rev. 144, 1 (1995).
47. T. J. Collins, R. D. Powell, C. Slebodnick, E. S. Uffelman, J. Am. Chem. Soc. 112, 899 (1990); M. K. Stern and J. T. Groves, in Manganese Redox Enzymes, V. L. Pecoraro, Ed. (VCH, New York, 1992), pp. 233–259.
48. D. T. Sawyer, Oxygen Chemistry, (Oxford Univ. Press, New York, 1991).

49. A. Chu, A. P. Nguyen, R. J. Debus, Biochemistry 34, 5859 (1995).
50. C. W. Hoganson and G. T. Babcock, in Metal Ions in Biological Systems, vol. 30, Metalloenzymes Involving Amino Acid-Residue and Related Radicals, H. Sigel and A. Sigel, Eds., (Dekker, New York, 1994), pp. 77–107.
51. W. H. Saunders Jr. and A. F. Cockerill, Mechanisms of Elimination Reactions (Wiley, New York, 1973).
52. G. T. Babcock, R. E. Blankenship, K. Sauer, FEBS Lett. 61, 286 (1976); M. R. Razeghifarad, C. Klughammer, R. J. Pace, Biochemistry 36, 86 (1997).
53. A. Boussac, P. Sétif, A. W. Rutherford, Biochemistry 31, 1224 (1992).
54. L. I. Krishtalik, Bioelectrochem. Bioenerg. 23, 249 (1990).
55. G. Tian, J. A. Berry, J. P. Klinman, Biochemistry 33, 226 (1994); J. P. Klinman, Chem. Rev. 96, 2541 (1996).
56. R. M. Wachter and B. P. Branchaud, J. Am. Chem. Soc. 118, 2782 (1996).
57. C. F. Yocum, Biochim. Biophys. Acta 1059, 1 (1991); H. Wincencjusz, H. J. van Gorkom, C. F. Yocum, Biochemistry 36, 3663 (1997).
58. B. E. Sturgeon et al., J. Am. Chem. Soc. 118, 7551 (1996).
59. Supported by NIH grant GM-37300 and the USDA Competitive Grants Office. We thank C. F. Yocum, C. Tommos, K. Warncke, N. Lydakis-Simantiris and M. Gardner for useful discussions.

26 October 1996; accepted 28 May 1997

▉ RESEARCH ARTICLE

Global Sea Floor Topography from Satellite Altimetry and Ship Depth Soundings

Walter H. F. Smith* and David T. Sandwell

A digital bathymetric map of the oceans with a horizontal resolution of 1 to 12 kilometers was derived by combining available depth soundings with high-resolution marine gravity information from the Geosat and ERS-1 spacecraft. Previous global bathymetric maps lacked features such as the 1600-kilometer-long Foundation Seamounts chain in the South Pacific. This map shows relations among the distributions of depth, sea floor area, and sea floor age that do not fit the predictions of deterministic models of subsidence due to lithosphere cooling but may be explained by a stochastic model in which randomly distributed reheating events warm the lithosphere and raise the ocean floor.

Knowledge of ocean floor topography data is essential for understanding physical oceanography, marine biology, chemistry, and geology. Currents, tides, mixing, and upwelling of nutrient-rich water are all influenced by topography. Seamounts may be

W. H. F. Smith is at the National Oceanic and Atmospheric Administration, Code E/OC-2, 1315 East-West Highway, Silver Spring, MD 20910–3282, USA.
D. T. Sandwell is at the Scripps Institution of Oceanography, La Jolla, CA 92093, USA.

*To whom correspondence should be addressed. E-mail: walter@amos.grdl.noaa.gov

particularly important in mixing and tidal dissipation (1), and deep water fisheries on seamount flanks have become economically significant (2). Seamounts, oceanic plateaus, and other geologic structures associated with intraplate volcanism, plate boundary processes, and the cooling and subsidence of the oceanic lithosphere should all be manifest in accurate bathymetric maps.

Conventional sea floor mapping is a tedious process. Ships have measured depth with single-beam echo sounders since the